



AEROELASTIC DIVERGENCE AND FREE VIBRATION OF TAPERED COMPOSITE WINGS

Mengchun Yu*, Chyanbin Hwu*

* National Cheng Kung University, Department of Aeronautics and Astronautics

Keywords: *aeroelastic, divergence, free vibration, wing, tapered, eigenvalue*

Abstract

In aeroelasticity, divergence of wing structures is an important static phenomenon. On the other hand, the free vibration analysis is significant to investigate the dynamic characteristics of the structure. Recently, a comprehensive wing model considering the airfoil shape was established. However, the analysis of tapered wing was still not taken into account so far. In this paper, this model is extended to discuss the tapered composite wings. By employing the Hamilton's principle and following the standard procedure of finite element formulation, an elementwise comprehensive model was developed. Because this model can be applied to both static and dynamic analyses, divergence and free vibration will be studied. In this model, aerodynamic force vector containing the lift and moment of the wings was approximated by the strip theory, which will then lead to a standard eigen-relation for solving the divergence dynamic pressure by neglecting the inertial terms. Besides, this model will also provide another eigen-relation for solving the natural frequencies when all the external forces are eliminated.

1 Introduction

The fundamental work concerning the divergence instability of swept metallic wings was done about fifty years ago. It was shown that low static aeroelastic divergence speeds were associated with the swept-forward wings unless they were stiffened enough. Because the metallic wing is limited to its material properties, the swept-forward wing aircraft was considered as an impossible task for a time. Until the aeroelastic tailoring concept for the composite wing structures was raised and studied by Krone [1], relevant research about swept composite wing sprouts once again.

Numerous different analytical model of the composite wing structures such as the classical beam model [2,3], the coupled bending-torsion model [4-6], and the refined models taking warping restraint [7-10], transverse shear deformation [11], shell bending strain [12,13], and cross-sectional materials and geometries [14,15] into account have been developed in the past several decades. However, they just treated the wing as plane beam without considering the airfoil shape due to the complexity. Recently, a comprehensive model considering the shape of airfoil for composite wing structures was therefore developed by our co-workers [16,17]. This model can treat the more realistic wing structures such as stiffened multicell wings that are composed of the laminated skins, stringers, ribs, and spars. No matter how comprehensive the model is, it is still restricted to the cases of the wings with uniform airfoil shape along span direction.

To study the tapered effect of the wing structure and to improve the computational efficiency of the comprehensive model, in this article the elementwise comprehensive model is derived from the Hamilton principle with the concept of finite element method embedded in. Both the accuracy and computational efficiency of the elementwise comprehensive model are compared with the results that are provided by the existing papers or the commercial finite element software packages (ANSYS) in the aeroelastic divergence and free vibration analyses.

2 Elementwise Comprehensive Model of Composite Wing

2.1 Assumptions and the Comprehensive Model

If the cover skin of the wing is made of composite laminates, the entire wing structure may be simulated as a composite sandwich plate [16,17] in which the wing skins, stringers, and spar flanges are simulated as the faces resisting the in-plane force and bending moment; furthermore, the spar webs

and ribs are simulated as the core resisting the transverse shear and the force normal to the face. With the transverse stiffening components, it is usually assumed that the wing chordwise section is strong enough to avoid the deformation. So that some aerodynamic parameters are constants as the airfoil shape of the wing is fixed. Besides, because the wing cross section must have a streamline shape commonly referred to as an airfoil section, the thickness of the sandwich will be a function of the airfoil and the thickness is not too small to neglect the transverse shear deformation. Based upon these considerations shown above, a comprehensive model was developed [17]. In this model, the displacement field can be expressed as follows:

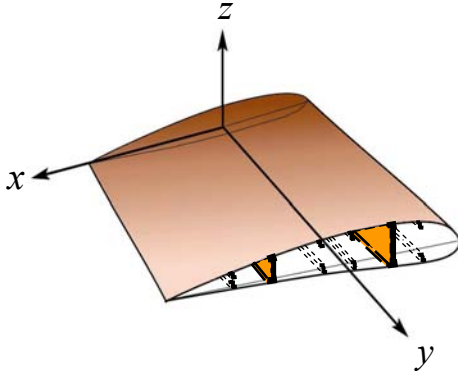


Fig. 1. Geometry of the composite wing [16]

$$u(x, y, z, t) = z\theta(y, t) \quad (1a)$$

$$v(x, y, z, t) = v_0(y, t) + z\{\beta_f(y, t) + x\beta_r(y, t)\} \quad (1b)$$

$$w(x, y, z, t) = w_f(y, t) - x\theta(y, t) \quad (1c)$$

where u , v , and w are the displacement components in the direction x (chordwise), y (spanwise), z (thicknesswise), respectively (Fig. 1); t is the time variable, v_0 the midplane displacement in the y direction, w_f the displacement (positive upward) in the z direction measured along the reference axis, and θ the rotation angle with respect to x axis due to twist around the reference axis (positive nose up), that is, $\beta_x = \theta$. Furthermore, β_f is the rotation angle of x - z plane with respect to the y axis measured at the reference axis and β_r is the variation rate of β_f along the x axis, hence $\beta_x = \beta_f + x\beta_r$. Through the above interpretation, it is obvious that there are five basic deformation functions for the stiffened composite wing structures as follows, v_0 , w_f , θ , β_f , and β_r . The equations of motion, constitutive equation, and

boundary conditions can be expressed in matrix form as follows:

$$\mathbf{F}' - \mathbf{F}_0 + \mathbf{p} = \mathbf{I}_0 \ddot{\mathbf{d}} \quad (2)$$

$$\mathbf{F} = \mathbf{K}_1 \mathbf{d} + \mathbf{K}_2 \mathbf{d}', \quad \mathbf{F}_0 = \mathbf{K}_0 \mathbf{d} + \mathbf{K}_1^T \mathbf{d}' \quad (3)$$

$$\mathbf{K}_1 \mathbf{d} + \mathbf{K}_2 \mathbf{d}' = \hat{\mathbf{F}} \text{ on } y = y_f \text{ and } y = y_0 \quad (4)$$

where \mathbf{F} , \mathbf{p} and \mathbf{d} are, respectively, the section force, surface force and displacement vectors; \mathbf{K}_0 , \mathbf{K}_1 and \mathbf{K}_2 are stiffness matrices related to the extensional, coupling and bending stiffness of the composites; \mathbf{I}_0 is a matrix related to the mass, gravity center and moment of inertia. The overdot and the prime denote, respectively, the differentiation with respect to time and space. The overhat stands for the prescribed value on the boundaries. Please refer to Hwu and Gai [17] for detailed explanation.

2.2 Deduction of the Elementwise Comprehensive Model

In order to refine the comprehensive model, the model is rederived from Hamilton's principle [18] as shown by the following equation:

$$\delta \int_{t_1}^{t_2} (\pi - \kappa) dt = 0 \quad (5a)$$

where π is potential energy consisting of strain energy and the work done by the body forces and surface tractions and κ is the kinetic energy as follows,

$$\pi = \int_V \left(\frac{1}{2} \sigma_{ij} \varepsilon_{ij} - f_i u_i \right) dV - \int_{S_\sigma} (\hat{T}_i u_i) dS \quad (5b)$$

$$\kappa = \frac{1}{2} \int_V \rho \dot{u}_i \dot{u}_i dV \quad (5c)$$

By introducing Eq. (3) into Eq. (5b) and (5c) and subtracting Eq. (5c) from Eq. (5b), we may obtain

$$\begin{aligned} \pi - \kappa &= \frac{1}{2} \int_y \left[\mathbf{d}'^T \mathbf{K}_2 \mathbf{d}' + 2 \mathbf{d}'^T \mathbf{K}_1 \mathbf{d} + \mathbf{d}^T \mathbf{K}_0 \mathbf{d} - \dot{\mathbf{d}}^T \mathbf{I}_0 \dot{\mathbf{d}} - 2 \mathbf{p}^T \mathbf{d} \right] dy \\ &\quad - \left[\hat{\mathbf{F}}^T \mathbf{d} \right]_{y_0}^{y_f} \end{aligned} \quad (6)$$

The governing equations and boundary conditions derived from Eq. (6) agree with Eq. (2) and Eq. (4) derived in [17].

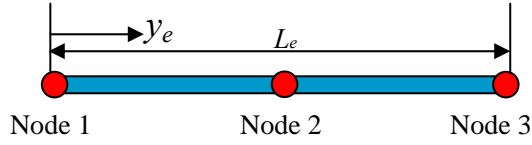


Fig. 2. Local coordinate of each element

Because y -axis is the primary coordinate variable in the wing structure. Thus the wing structures are simulated as a beam divided in n elements connected along the y axis. Each element has 3 nodes (Fig. 2) and the shape function of each node is expressed by 2nd order polynomials. By following the procedures stated between eqns.(5)-(6), the energy expression of each element can be written in terms of the nodal displacement vector \mathbf{u}_e as

$$\pi - \kappa = \int_{y_e} \left\{ \frac{1}{2} \mathbf{u}_e^T \left[g^2 \mathbf{K}_e - \dot{g}^2 \mathbf{J}_e \right] \mathbf{u}_e - g(t) \mathbf{u}_e^T \mathbf{f}_e \right\} dy \quad (7)$$

in which g is a function of time, and \mathbf{K}_e , \mathbf{J}_e and \mathbf{f}_e are, respectively, element stiffness matrix, element inertia matrix and element external force vector determined through the following relations:

$$\mathbf{K}_e = \int_{y_e} \left\{ \mathbf{N}^T \mathbf{K}_2 \mathbf{N}' + 2 \mathbf{N}^T \mathbf{K}_1^T \mathbf{N}' + \mathbf{N}^T \mathbf{K}_0 \mathbf{N} \right\} dy \quad (8a)$$

$$\mathbf{J}_e = \frac{1}{2} \int_{y_e} \mathbf{N}^T \mathbf{I}_0 \mathbf{N} dy \quad (8b)$$

$$\mathbf{f}_e = \frac{1}{2} \int_{y_e} \mathbf{N}^T \mathbf{p} dy + \left[\mathbf{N}^T \hat{\mathbf{F}} \right]_{y_0}^{y_f} \quad (8c)$$

where $\mathbf{N}(y)$ is the shape function matrix.

2.2.1 Divergence

In this article, we will use the aerodynamic strip theory and the known results for two-dimensional flow to approximate the lift and the pitching moment [19]. The relation between the structure deformation and aerodynamic forces (lift force L and pitching moment T) can be expressed as

$$L(y) = q_n \left[ac \theta_0 + ac(\theta(y) - w'_f \tan \Lambda) \right] \quad (9a)$$

$$T(y) = q_n \left[ace \theta_0 + c^2 C_{m,ac} \right] + ac(e \theta(y) - ew'_f \tan \Lambda) \quad (9b)$$

where c is the chord length, θ_0 the initial angle of attack, $C_{m,ac}$ the pitching moment coefficient about the aerodynamic center, and e the distance between the lines of aerodynamic and flexural centers. The normal dynamic pressure q_n is

$$q_n \equiv \frac{1}{2} \rho V_n^2 = q \cos^2 \Lambda \quad (10)$$

where ρ , V_n , q , and Λ are the density of the airflow, airflow velocity normal to the leading edge, dynamic pressure, and the angle of sweep respectively. The lift curve slope coefficient a is an aerodynamic parameter defined as

$$a \equiv \frac{dC_L}{d\alpha} = a_0 \frac{AR}{AR + 4 \cos \Lambda} \quad (11)$$

where a_0 is the corresponding 2D lift curve slope and AR is the aspect ratio.

With the aerodynamic functions listed above, the external aerodynamic force vector \mathbf{f}_e can be simplified further as

$$\mathbf{f}_e = \int \mathbf{N}^T(y) \mathbf{p}(y) dy = q_n (\mathbf{p}_0 + \mathbf{K}_a \mathbf{u}_e) \quad (12)$$

where the value of \mathbf{p}_0 is constant, but the value of the aerodynamic stiffness matrix \mathbf{K}_a varies with the interaction between the aerodynamics (L , T) and the displacement function (\mathbf{u}_e).

Because divergence is a static phenomenon in aeroelasticity, we can neglect the time effect by eliminating the inertial terms \mathbf{J}_e . Equation (7) can therefore be rewritten as follows

$$\pi - \kappa = \frac{1}{2} \mathbf{u}_e^T \mathbf{K}_e \mathbf{u}_e - \mathbf{u}_e^T q_n (\mathbf{p}_0 + \mathbf{K}_a \mathbf{u}_e) \quad (13)$$

After substituting Eq. (13) into Eq. (5a), the equilibrium equation of the divergence analysis is expressed as

$$\left[\frac{1}{2} (\mathbf{K}_e + \mathbf{K}_e^T) - q_n (\mathbf{K}_a + \mathbf{K}_a^T) \right] \mathbf{u}_e = q_n \mathbf{p}_0 \quad (14)$$

The determinant of the coefficient matrix of \mathbf{u}_e should be zero to avoid the trivial solutions, which will then lead to the result of divergence,

$$\left\| \frac{1}{2} (\mathbf{K}_e + \mathbf{K}_e^T) - q_n (\mathbf{K}_a + \mathbf{K}_a^T) \right\| = 0 \quad (15)$$

Obviously, it is an eigen problem and the eigenvalue and eigen-vector indicate the normal divergence dynamic pressure and the nodal displacement vector respectively. After the superposition of all the elements accomplishing, the eigen problem can be solved.

2.2.2 Free Vibration

To determine the natural frequency of the stiffened wing structures, the values of all components in the body force distribution vector $\tilde{\mathbf{p}}$ and the prescribed surface traction \hat{T}_i are both set as zero in the equation. So that the element external force vector can be expressed as $\mathbf{f}_e = \mathbf{0}$. Furthermore, $g(t)$ is assumed as a harmonic motion with the natural frequency ω in the free vibration analysis. By using Eq. (7) and Hamilton's principle again, the equation of motion is derived as

$$\frac{1}{2}[(\mathbf{K}_e + \mathbf{K}_e^T) + \omega^2(\mathbf{J}_e + \mathbf{J}_e^T)]\mathbf{u}_e = \mathbf{0} \quad (16)$$

The nontrivial solutions of Eq. (16) exist only when the determinant of the coefficient matrix of \mathbf{u}_e becomes zero, which will then provide us the following equation for solving natural frequencies:

$$\left\| \frac{1}{2}(\mathbf{K}_e + \mathbf{K}_e^T) + \omega^2 \frac{1}{2}(\mathbf{M}_e + \mathbf{M}_e^T) \right\| = 0 \quad (17)$$

As shown above, it is also an eigen problem and the eigen-value and eigen-vector indicate the square of natural frequency and the nodal displacement vector respectively. After the superposition of all the elements accomplishing, the eigen problem can be solved. It is similar to the divergence analysis.

3 Numerical Results

3.1 Divergence

In this section, the calculating efficiency of the elementwise comprehensive model will be shown first. And the accuracy of the present model will be examined by comparing with the existing numerical solutions provided by other papers.

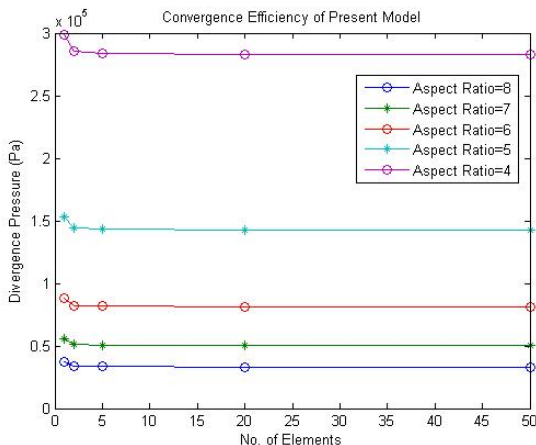


Fig. 3. Convergence study of the present model

As shown in Fig. 3, even the wing is just divided into few elements, the divergence dynamic pressures (of different aspect ratio) calculated by the elementwise comprehensive model still converge very rapidly. To further examine the computational efficiency, the example of composite wing structure with NACA 2412 airfoil used by Hwu and Tsai [16] is adopted here. The present method only spends 1/10 of the time consumed in Ref. [16].

Next, the accuracy of present model is checked by comparing with the results of the uniform metallic wing structure (without tapered) evaluated by Weisshaar [20] and Librescu [21]. As shown in Fig. 4, the present data also agree with them especially when $AR = 4$. Besides, Fig. 4 also reveals that the divergence dynamic pressure will decrease as the values of aspect ratio AR increase.

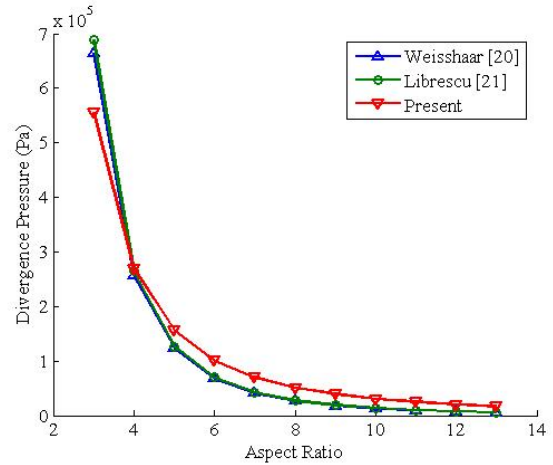


Fig. 4. Comparison with the existing data

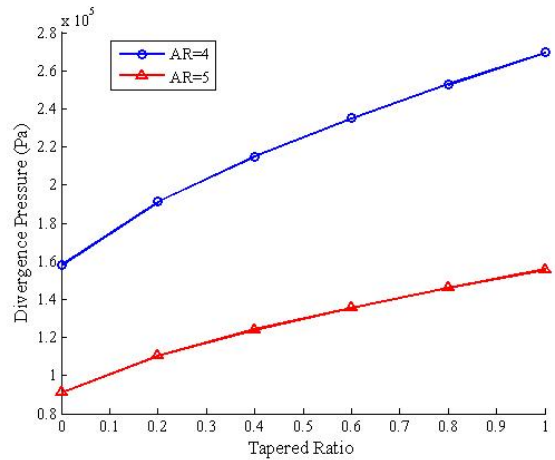


Fig. 5. Tapered effect in aeroelastic divergence of the wing structure

Before investigating the tapered effect in wing structures, the taper ratio r_t is denoted as

$$r_t = \frac{c_{root} - c_{tip}}{c_{root}} \quad (18)$$

where c_{root} and c_{tip} are the chord lengths of the wing root and wing tip, respectively.

The examples in a series of tapered ratios are solved for $AR = 4$ and 5 . The numerical results are shown in Fig. 5. It shows that once the value of tapered ratio increases, the value of divergence pressure will increase, too.

3.2 Free Vibration

In this section, the present model is first examined by comparison with the existing numerical data of the wing structure with uniform span evaluated by Hwu and Gai [17]. The geometry properties of the wing are chordwise length $c=0.1\text{m}$ and spanwise length $L=0.4\text{m}$ shown in Fig. 6 (with $c_{root} = c_{tip}$) where c_{root} and c_{tip} means the chord length at the wing root and wing tip respectively. The detailed material properties of wing are listed in [17].

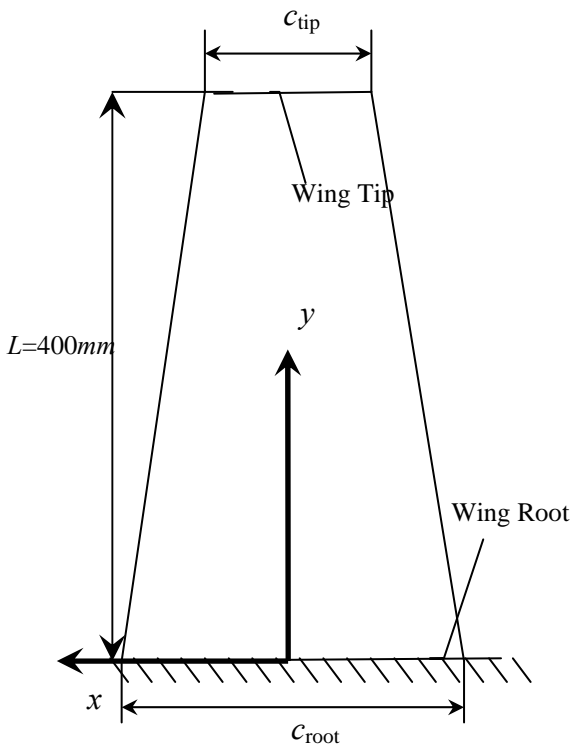


Fig. 6. Geometry of the tapered composite wing

Table 1 shows the natural frequencies got from the present model in this article well agree with the solution of Hwu & Gai and ANSYS. It deserves to be mentioned that the calculating efficiency is also improved as shown in Table 2.

Table 1. Natural frequencies comparison for the wing structure with uniform span (Unit:Hz)

Mode No.	Present	Hwu & Gai [17]	ANSYS
I	16.89	16.15	15.75
II	99.12	96.45	93.84
III	108.69	110.34	114.94
IV	256.83	252.45	245.18
V	325.23	333.85	343.82

Table 2. Time consumed comparison

	Present	Hwu & Gai [17]	ANSYS
Time consumed (minute)	2	25	30

Table 3. Effects of the taper ratio on the basic natural frequencies (Mode I) (Unit:Hz)

Taper ratio	Mode No.	Present	ANSYS
1.0	I	16.89	15.25
	II	99.12	90.35
	III	108.69	113.16
	IV	256.83	234.64
	V	325.23	275.61
0.95	I	17.38	14.37
	II	99.88	85.11
	III	113.85	117.66
	IV	256.83	224.07
	V	330.82	280.47
0.80	I	19.08	16.47
	II	101.88	88.43
	III	132.73	125.47
	IV	256.89	224.35
	V	350.35	277.64
0.70	I	20.49	17.13
	II	103.39	87.02
	III	148.41	133.02
	IV	257.09	217.85
	V	366.40	271.96
0.60	I	22.21	17.91
	II	105.23	85.39
	III	167.08	155.67
	IV	257.58	210.67
	V	385.92	268.10
0.20	I	35.50	22.90
	II	122.80	80.28
	III	267.76	120.55
	IV	282.12	180.53
	V	465.98	213.95

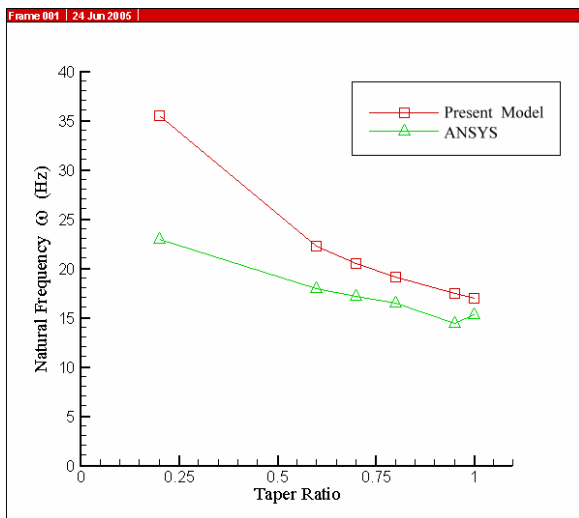


Fig. 7. The trend of the natural frequency (Mode I)

Then we consider a tapered composite wing structure with NACA 2412 airfoil and the same material properties as the preceding example. But the values of taper ratio are set as a series of values 1.00, 0.95, 0.80, 0.70, 0.60, and 0.20. In order to check the accuracy, the natural frequencies are evaluated in two ways, the present model and ANSYS. The results of the present model do not agree well with ANSYS shown in Table 3. The difference may result from that the mesh-process encounter something trouble for the geometry variation (tapered wing). However, we observe a trend that the basic natural frequency will increase when the taper ratio r_t decrease, as shown in Fig. 7.

4 Conclusion

By embedding the finite element formulation in the comprehensive model [17], the elementwise model in this article can deal generally with the uniform and tapered composite wing structures. Besides, the excellent calculating efficiency saves a lot of computational time that is consumed before.

The divergence analysis and the free vibration analysis both are eigen-value problems. With the usual procedure for finite element formulation, the eigenvalue such as divergence dynamic pressure and the natural frequencies could be solved similarly. It can also be observed that the divergence dynamic pressure will increase but the fundamental natural frequency will decrease when the taper ratio r_t increases.

References

[1] Krone, Jr. N. J. "Divergence elimination with advanced composites". *AIAA Paper 75-1009*, L.A.,CA., 1975

- [2] Bisplinghoff, R. L., Asheley, H., and Halfman, R. L., "Aeroelasticity". Addison-Wesley, Cambridge, MA, Chaps. 2 and 3, 1955.
- [3] Megson, T. H. G., "Aircraft structures-for engineering students". 2nd ed., Edward Arnold, London, Chap. 8, 1990.
- [4] Weisshaar, T. A. , and Foist, B. L. , "Vibration tailoring of advanced composite lifting surfaces," *Journal of Aircraft*, Vol. 22, pp.141-147, 1985.
- [5] Chandra, R., Stemple, A. D., and Chopra, I., "Thin-walled composite beams under bending, torsional, and extensional loads," *Journal of Aircraft*, Vol. 27, pp.619-626, 1990.
- [6] Banerjee, J. R., and Williams, F. W., "Free vibration of composite beams: an exact method using symbolic computation," *Journal of Aircraft*, Vol. 32, No. 3, pp.636-642, 1995.
- [7] Crawley, E. F., and Dugundji, J., "Frequency determination and nondimensionalization for composite cantilever plates," *Journal of Sound and Vibration*, Vol. 72, No. 1, pp. 1-10, 1980.
- [8] Lottati, I., "Flutter and divergence aeroelastic characteristics for composite forward swept cantilevered wing," *Journal of Aircraft*, Vol. 22, No.11, pp. 1-10, 1985.
- [9] Librescu, L., and Khdeir, A.A., "Aeroelastic divergence of swept-forward composite wings including warping restraint effect," *AIAA Journal*, Vol. 26, No. 11, pp. 1373-1377, 1988.
- [10] Oyibo, G. A. and Bentson, J., "Exact solutions to oscillations of composite aircraft wings with warping constraint and elastic coupling" *AIAA*, Vol.28, No. 6, pp.1075-1081, 1990.
- [11] Librescu, L., and Song, O., "On the static aeroelastic tailoring of composite aircraft swept wings modelled as thin-walled beams structures," *Composite Engineering*, Special Issue, Use of Composite in Rotor Craft and Smart Structures, Vol. 2, No. 5-7, pp. 497-512, 1992.
- [12] Volovoi, V. V., and Hodges, D. H., "Single- and multicelled composite thin-walled beams," *AIAA Journal*, Vol. 40, No. 5, pp. 960-965, 2002.
- [13] Volovoi, V. V., and Hodges, D. H., "Theory of anisotropic thin-walled beams," *Journal of Applied Mechanics*, Vol. 67, No. 3, pp. 453-459, 2000.
- [14] Yu, W., Volovoi, V. V., Hodges, D. H., and Hong, X., "Validation of the variational asymptotic beam sectional analysis," *AIAA Journal*, Vol. 40, No. 10, pp. 2105-2112, 2002.
- [15] Yu, W. , Hodges, D. H., Volovoi, V. V., and Cesnik, C.E.S., "On Timoshenko-like modeling of initially curved and twisted composite beams," *International Journal of Solids and Structures*, Vol. 39, pp. 5101-5121, 2002.

- [16] Hwu, C. and Tsai, "Aeroelastic divergence of stiffened composite multicell wing structures," *Journal of Aircraft*, Vol.39, No. 2, pp.242-251, 2002.
- [17] Hwu, C. and H.S. Gai, "Vibration analysis of composite wing structures by a matrix form comprehensive model," *AIAA Journal*, Vol.41, No.11, pp.2261-2273, 1997.
- [18] Clough, R.W. and Penzien, J., "*Dynamics of structures*", McGraw-Hill, New York, 1993.
- [19] Oyibo, G. A., "Generic approach to determine optimum aeroelastic characteristics for composite forward-swept-wing aircraft," *AIAA Journal*, Vol.22, No.1, pp.117-123, 1984.
- [20] Weisshaar, T. A., "Divergence of forward swept composite wings," *Journal of Aircraft*, Vol.17, No. 6, pp.442-448, 1980.
- [21] Librescu, L., and Simovich J., "General formulation for the aeroelastic divergence of composite swept-forward wing structures," *Journal of Aircraft*, Vol.25, No. 4, pp.364-371, 1988.